SPACE DISTRIBUTION AND LUMINOSITY FUNCTIONS OF QUASI-STELLAR RADIO SOURCES

MAARTEN SCHMIDT
Mount Wilson and Palomar Observatories, Carnegie Institution of Washington,
California Institute of Technology
Received July 18, 1967; revised August 21, 1967

ABSTRACT

The distribution in space and both the optical and radio luminosity functions of quasi-stellar radio sources are derived The derivation is based on quasi-stellar sources in the *Revised 3C Catalogue*, in which they have been identified and observed with a high degree of completeness down to magnitude around $18\frac{1}{2}$. The redshifts are assumed to be cosmological. The distribution in space is found to be strongly non-uniform. The space density, in co-moving coordinates, is increasing with redshift z, such that at $z = 1$ the density is around 150 and 80 times the local $(z = 0)$ density, for $q_0 = 0$ and $q_0 = 1$, respectively. This density increase corresponds to a $N(S)$ relation quite similar to that exhibited by extragalactic radio sources.

The optical luminosity function is relatively flat, i e., the numbers per magnitude depend little on the luminosity In contrast the radio luminosity function is rather steep, the number per magnitude increasing toward fainter radio luminosities by a factor of around three to four per magnitude. Extension of this radio luminosity function by $1\frac{1}{2}$ magnitude is sufficient to account for the Sandage-Luyten estimate of the sky density of quasi-stellar objects. The local $(z = 0)$ density of quasi-stellar objects can then be estimated at 7×10^{-9} and 12×10^{-9} Mpc^{-3}, for $q_0 = 0$ and $q_0 = 1$, respectively.

Unpublished spectra and redshifts of quasi-stellar sources are given in the Appendix.

I. INTRODUCTION

The present paper describes a study of the space distribution and the optical and radio luminosity functions of quasi-stellar radio sources. The relation between these functions and the observable properties of the quasi-stellar sources (QSS) is particularly complicated due to selection effects in both optical and radio data.

The relation between optical or radio flux density and redshift has been discussed by Heidmann (1966), Hoyle and Burbidge (1966), Bolton (1966), Longair (1966b), Sciama and Rees (1966), Roeder and Mitchell (1966), Rowan-Robinson (1966), and McVittie and Stabell (1967). Kafka (1967a) has stressed the importance of the radio selection effects and more recently (Kafka 1967b) also that of the optical selection effects.

The derivation of the space distribution and luminosity functions should be based on a sample of sources that is complete down to given limits of radio and optical flux density. An approximately complete sample of QSS is now available from identifications in the *Revised 3C Catalogue of Radio Sources* (Bennett 1962). The *Catalogue* is essentially complete down to 9 flux units at 178 Mc/s. Exhaustive identifications of QSS have been summarized by Wyndham (1966) and Véron (1966). Photometric and spectroscopic work has led to the rejection of a number of the proposed identifications (Sandage and Schmidt 1967). There remain forty-four identified QSS. Redshift and photometric data exist for forty sources[1] listed in Table 1 (see below). We use thirty-three of these sources as a sample essentially complete down to a specific optical flux density, as discussed in § VI.

The redshifts are assumed to be cosmological. The density distribution is investigated through a parameter V/V_m, explained in § VI, which for each source gives a measure of its position within the maximum volume over which it would be observable in the complete sample. This method has the advantage of being independent of the optical and

---

[1] No lines have been found in the spectra of 3C 93 and 3C 216; no spectra are available yet of the very faint sources 3C 43 and 3C 119

393

radio luminosity functions. Following the investigation of the density distribution, the luminosity functions are derived in § VII.

The large range of redshifts makes it imperative to establish a system of flux densities at a specific frequency at emission, over a fixed band width at emission. These systems are discussed in §§ IV and V. The optical continuum and the strengths of some emission lines are discussed in § III.

II. REDSHIFTS

Table 1 gives the redshifts of forty QSS in the *3CR Catalogue*. The data have been collected from Greenstein and Matthews (1963), Schmidt (1963, 1965, 1966), Schmidt and Matthews (1964), Burbidge (1965, 1966), Lynds, Stockton, and Livingston (1965), Oke (1965), Burbidge and Kinman (1966), Burbidge, Lynds, and Burbidge (1966), Ford and Rubin (1966), Hiltner, Cowley, and Schild (1966), Lynds, Hill, Heere, and Stockton (1966), Stockton and Lynds (1966), Dibai and Esipov (1967), and Lynds (1967). The redshifts of 3C 205, 3C 268.4, 3C 288.1, and 3C 323.1 are new; the spectral data are given in the Appendix, together with further as yet unpublished redshift data obtained for other QSS. The values of the redshifts used are usually the average of published values that were available in October, 1966. In general, different observers show good agreement in line identifications and redshifts. The redshift of 3C 263 depends on only one emission line; its identification as Mg II $\lambda2798$ by Ford and Rubin (1966) is most likely correct. The redshifts of all other sources depend on at least two emission lines.

III. EFFECT OF EMISSION LINES ON OPTICAL MAGNITUDES

Magnitudes and colors of the forty 3CR QSS with redshifts are given in Table 1. They are all due to Sandage (1965, 1966, 1967). The observed UBV values should be corrected for the effect of galactic absorption and for that of the emission lines in the source spectrum. The following corrections for galactic absorption were applied:

$$\Delta V = -0^{m}18 \operatorname{cosec} b \,,$$

$$\Delta(B - V) = -0^{m}06 \operatorname{cosec} b \,,$$

$$\Delta(U - B) = 0\ 72\ \Delta(B - V) \,.$$

(1)

Following Sandage (1965), we adopt for the low-latitude sources 3C 138, 3C 147, and 3C 175 a correction $\Delta V = -0.9$ mag and corresponding corrections to $B - V$ and $U - B$.

The correction for the effect of the emission lines is required since we wish to derive a flux density at a fixed emitted wavelength, by interpolation or extrapolation from the UBV magnitudes. Ideally, the strengths of the emission lines should be determined for every source individually, but these have been measured for a few sources only. Hence, we attempt a statistical correction, following the suggestions by Lynds (1966) and Strittmatter and Burbidge (1967) that the emission lines are responsible for the variation of $(U - B)$ and $(B - V)$ with redshift z (Sandage 1966).

We used for this study sixty-four quasi-stellar radio sources for which redshifts and photometry were available in October, 1966. Figure 1 shows their colors, after correction for galactic reddening, as a function of the redshift. We adopt for the effective transmission functions $S(\lambda)$ of the UBV system the values given under "$S(\lambda)_1$, 1 Air Mass" in Table A1 of Matthews and Sandage (1963). If E is the equivalent width of an emission line (observed wavelength λ_e) in wavelength units, then the effect of the line on the observed magnitude is easily written as

$$\Delta m \simeq \frac{ES(\lambda_e)}{\int S(\lambda)\,d\lambda} \,.$$

(2)

Here it has been assumed that the line is much narrower than the filter transmission width, that it is not very strong relative to the continuum, and that the continuum flux density per unit wavelength is rather flat across the filter transmission width. The errors introduced by these approximations are expected to be much smaller than those corresponding to the scatter of the points in Figure 1.

If the rest wavelength of the emission line is λ_0, then

$$\lambda_e = \lambda_0(1 + z) , \qquad E = E_0(1 + z) , \tag{3}$$

where E_0 is the equivalent width at rest.

We have only considered the effect of the emission lines of Mg II $\lambda 2798$ Å and C IV $\lambda 1549$ Å. We illustrate the procedure by considering the effect of Mg II emission on the $U - B$ colors. For redshifts up to $z = 0.93$ it is the only major line affecting $U - B$.

TABLE 1

PHOTOMETRIC AND RADIO DATA FOR 40 3CR SOURCES WITH REDSHIFTS

Source	z	V	$B-V$	$U-B$	log $f(2500)$	$S(178)$	α	log $f(500)$
3C 273 .	0 158	12 80	+0 21	−0 85	−27 63	67	−0 26	−24 27
323 1	0 264	16 69	+ 11	−0 85	29 17	9 0	−0 66	25 32
249 1	0 311	15 72	− 02	−0 77	28 75	11 5	−0 89	25 29
277 1	0 320	17 93	− 17	−0 78	29 62	12 0	−0 94	25 29
48	0 367	16 20	+ 42	−0 58	29 12	47	−0 44	24 54
351	0 371	15 28	+ 13	−0 75	28 61	11 0	−0 63	25 22
215 ..	0 411	18 27	+ 21	−0 66	29 84	10 0	−1 01	25 39
47	0 425	18 10	+ 05	−0 65	29 74	20	−0 72	25 00
147	0 545	17 80	+ 65	−0 37	29 57	58	−0 47	24 48
334	0 555	16 41	+ 12	−0 59	29 12	10 0	−0 73	25 32
275 1	0 557	19 00	+ 23	−0 43	30 29	16 0	−0 91	25 16
345	0 594	15 96	+ 29	−0 50	29 02	10 0	−0 28	25 21
263	0 643	16 32	+ 18	−0 56	29 14	13 0	−0 75	25 21
207	0 683	18 15	+ 43	−0 42	29 91	10 0	−0 72	25 32
380	0 691	16 81	+ 24	−0 59	29 24	57	−0 72	24 57
254	0 734	17 98	+ 15	−0 49	29 80	19 0	−0 90	25 09
138	0 759	18 84	+ 53	−0 16	29 91	18 5	−0 37	24 99
175 .	0 768	16 60	+ 46	−0 51	28 99	16 0	−0 92	25 17
286 .	0 848	17 30	+ 22	−0 84	29 57	21	−0 05	24 89
454 3	0 860	16 10	+ 47	−0 66	29 12	15 0	−0 20	25 06
196	0 871	17 60	+ 60	−0 46	29 74	59	−0 72	24 56
309 1	0 905	16 78	+ 46	−0 77	29 39	17 0	−0 36	25 05
336	0 927	17 47	+ 44	−0 79	29 67	13 5	−0 89	25 24
288 1	0 961	18 12	+ 39	−0 82	29 95	9 5	−0 94	25 40
245	1 029	17 25	+ 45	−0 83	29 61	9 5	−0 52	25 34
2	1 037	19 35	+ 79	−0 96	30 51	15	−0 80	25 18
287	1 055	17 67	+ 63	−0 65	29 81	14 0	−0 33	25 15
186	1 063	17 60	+ 45	−0 71	29 66	13 5	−1 21	25 28
208	1 109	17 42	+ 34	−1 00	29 63	16 0	−0 84	25 16
204	1 112	18 21	+ 55	−0 99	29 96	9 5	−1 07	25 42
181	1 382	18 92	+ 43	−1 02	30 06	13 0	−0 96	25 27
268 4	1 400	18 42	+ 58	−0 69	30 16	9 0	−0 73	25 41
298	1 439	16 79	+ 33	−0 70	29 41	44	−0 99	24 74
270 1	1 519	18 61	+ 19	−0 61	30 15	12 0	−0 71	25 29
205	1 534	17 62	+ 49	−0 49	29 71	12 5	−0 91	25 28
280 1	1 659	19 44	− 13	−0 70	30 49	11 0	−1 11	25 35
454	1 757	18 40	+ 12	−0 95	30 02	9 0	−0 76	25 43
432	1 805	17 96	+ 22	−0 79	29 79	11 5	−1 06	25 33
191	1 952	18 40	+ 25	−0 84	29 96	10 5	−0 83	25 37
9	2 012	18 21	+0 24	−0 76	−29 98	15 0	−1 04	25 21

For each source we write $U - B = (U - B)_c - E_0 g(z)$, where $(U - B)_c$ is the mean continuum $U - B$ color and $g(z)$ is easily computed for each source from equations (2) and (3). A least-squares solution from thirty-eight $U - B$ values available up to $z = 0.93$ yields $(U - B)_c = -0.75$ and E_0 (Mg II) $= 76$ Å. Similar solutions can be made from the $B - V$ colors for the Mg II line, and from both colors for the C IV line. The results are given in Table 2 together with several determinations of continuum colors from ranges of redshift over which two filters are free of major lines.

The $(B - V)_c$ values for redshifts larger than 0.4 and the $(U - B)_c$ values at all redshifts show a remarkable independence of redshift. This can be most easily understood if the energy distribution of the continuum obeys a power law. We compute $a = \log f(\nu)/d \log \nu$ from the colors through (Sandage 1966)

$$a_1 = 0.38 - 4.08(B - V) , \qquad a_2 = -4.14 - 4.54(U - B) . \tag{4}$$

The continuum colors given in Table 2 yield values of a between -0.5 and -0.8. We
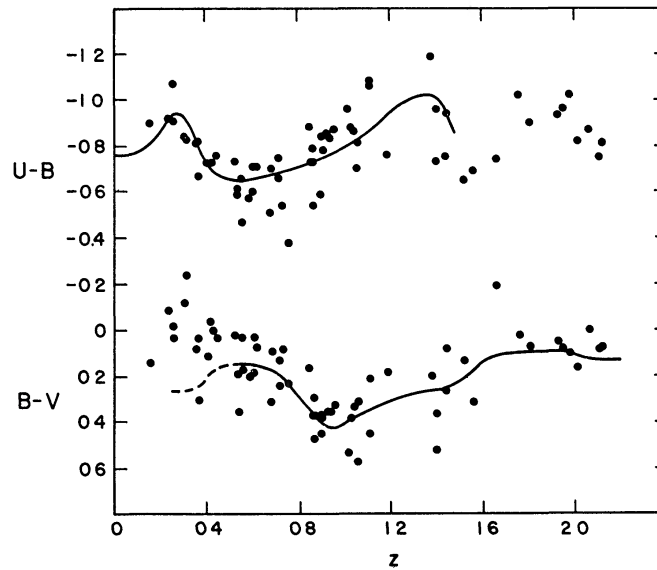

Fig. 1.—A diagram of $U - B$ and $B - V$ (corrected for galactic reddening) against redshift z for 64 QSS. The lines indicate the relation expected for a continuum $f(\nu) \sim \nu^{-0.7}$, with the emission lines of Mg II and C IV of rest equivalent widths of 74 and 62 Å, respectively. The dashed part of the curve corresponds to the apparent deviation above 3700 Å of the continuum from the power law.

TABLE 2

CONTINUUM COLORS AND EMISSION LINE STRENGTHS

z Range Used	Number of Colors Used	$(U-B)_c$	$(B-V)_c$	$(U-V)_c$	E_0(Mg II)	E_0(C IV)
0 15–0 93	38	−0 75	. ..		76 Å	.
0 5 –1 2	34	. ..	+0 25		72 Å	. .
0 89–1 66	22	−0 80	. .			35 Å
1 06–2 12	21		+0 26			81 Å
0 2 –0 4	8		0 00			
0 4 –0 8	19	. ..	.	−0 51		
0 8 –1 04	14	−0 80	. ..			
1 2 –1 5	5		+0 28			

have adopted an energy distribution $f(\nu) \sim \nu^{-0.7}$, corresponding to $(U - B)_c = -0.76$ and $(B - V)_c = +0.26$.

The low value of $(B - V)_c$ for redshifts below 0.4 cannot be explained by the relatively weak emission lines of [Ne v] and [O ii]. It is probably caused by a deficiency of intensity at rest wavelengths above 3700 Å, relative to the power law derived above. Table 3 gives some values of $f(\nu)$ relative to its value at $\nu = 1.2 \times 10^{15}$ c/s, or $\lambda = 2500$ Å.

The two values of the rest equivalent width of Mg ii given in Table 2 agree quite well; this does not support the suggestion by Strittmatter and Burbidge (1967) that the equivalent width of Mg ii is smaller for larger redshifts. The E_0 values for C iv determined from $U - B$ and $B - V$ are in poor agreement.

TABLE 3

CONTINUUM SPECTRUM OF AN AVERAGE QSS NORMALIZED TO 2500 Å

λ(Å)	1500	2000	2500	3000	3500	4000	4500
$f(\nu)/f(1.2 \times 10^{15}$ c/s) ..	0 70	0 86	1	1 13	1 26	1 2	1 0

TABLE 4

AVERAGE EFFECT OF MG II EMISSION ON UBV MAGNITUDES

z	ΔU	ΔB	z	ΔB	ΔV
0 0	0 00	.	0 8	0 05	0 07
.1	01	.	0 9	02	16
2	.10	. ...	1 0	0 00	.14
3	17	0 00	1 1	.	09
4	04	06	1 2.		04
5	0 00	11	1 3.		.01
6	.	11	1 4		01
0 7	...	0 08	1 5		0 00

The lines drawn in Figure 1 correspond to E_0 (Mg ii) $= 74$ Å and E_0 (C iv) $= 62$ Å. Although the main features are represented, there are considerable deviations from the curves. These are probably caused by a different behavior of both continuum and lines.

Our rest equivalent width of Mg ii of 74 Å is within the range of equivalent widths found by Oke (1966) from detailed spectrophotometry of several sources. Our equivalent width for C iv of 62 Å is smaller than values of 98 and 230 Å found by Oke for two sources. Fortunately, we only have to use filter magnitudes that require correction for the Mg ii emission, in a procedure described in the next section. Table 4 lists the effect of Mg ii emission on U, B, and V as a function of redshift.

IV. OPTICAL FLUX DENSITIES

Ideally, we would like to use the bolometric flux densities of the QSS, which is obviously impossible at present. The nearest and most practical approximation of the bolometric flux density is the monochromatic flux density $f_{em}(\nu)$ measured at a given emitted frequency ν over a band width of 1 c/s emitted. Since $f_{em}(\nu)$ represents a redshift-independent fraction of the bolometric flux density, the relation between $f_{em}(\nu)$, the total flux $F_{em}(\nu)$, and the redshift for different cosmological models is identical to that of the corresponding bolometric properties.

The choice of a standard emitted frequency is difficult due to the large range of redshifts. We have used 1.2×10^{15} c/s, corresponding to 2500 Å. This wavelength is free of emission lines and lies near the middle of the range 1500 Å to 3700 Å over which $f(\nu)$ follows the power law $\nu^{-0.7}$ according to the preceding section. At least one of the U, B, or V filters will measure within that range of rest wavelengths for redshifts from 0 to around 2.5.

Matthews and Sandage (1963) give the flux density at 4409 Å of a star of magnitude $B = 0$ with a power law spectrum with exponent -0.7 as 4.19×10^{-23} W m^{-2} (c/s)$^{-1}$. Remembering that this power law corresponds to $U - B = -0.76$, we find[2]

$$\log f_{\text{obs}}(3594) = -22.74 - 0.4\, U_c,$$

$$\log f_{\text{obs}}(4409) = -22.38 - 0.4\, B_c,$$ (5)

$$\log f_{\text{obs}}(5517) = -22.41 - 0.4\, V_c,$$

where U_c, B_c, and V_c are the magnitudes corresponding to the continuum, as discussed in § III.

We are interested in obtaining the observed flux density at 2500 $(1 + z)$ Å. If the redshift is such that, say, the V filter measures a rest wavelength between 1500 and 3700 Å, then

$$f_{\text{obs}}[2500(1+z)] = \left[\frac{2500(1+z)}{5517}\right]^{0.7} \times f_{\text{obs}}(5517).$$

Since 1 c/s emitted is observed as $(1 + z)^{-1}$ c/s, we have $f_{\text{em}}(2500) = (1 + z)^{-1} f_{\text{obs}}[2500(1 + z)]$. A similar derivation for the other filters yields

$$\log f_{\text{em}}(2500) = -22.85 - 0.4\, U_c - 0.3 \log (1 + z)$$

$$= -22.55 - 0.4\, B_c - 0.3 \log (1 + z)$$ (6)

$$= -22.66 - 0.4\, V_c - 0.3 \log (1 + z).$$

These equations apply *only* for those filters in the wavelength range 1500 $(1 + z)$ Å to 3700 $(1 + z)$ Å.

If for a source only one filter falls in this range, the value of $\log f_{\text{em}}(2500)$ so computed has been adopted. In all other cases it has been computed by interpolation according to $\log \nu$ between the two filters on either side of 2500 $(1 + z)$ Å. Table 1 lists for each source the value of $\log f_{\text{em}}(2500)$, henceforth to be denoted as $\log f(2500)$. Figure 2 shows the redshift-magnitude diagram for the forty 3CR sources.

V. RADIO FLUX DENSITIES

The procedure followed in deriving radio flux densities at a fixed emitted frequency is practically identical with that discussed in the preceding section. The fixed emission frequency was chosen at 500 Mc/s.

Values of the radio spectral index $\alpha = d \log S(\nu)/d \log \nu$ were derived for each source from the flux densities at 178 Mc/s in the *3CR* and those given by Kellermann (1964) at 400 Mc/s and Pauliny-Toth, Wade, and Heeschen (1966) at 750 Mc/s. We follow these authors in adopting a correction of $+16$ per cent to the flux densities given in the *3CR*. From these data we compute the observed flux density at 500 $(1 + z)^{-1}$ Mc/s, and divide by the band-width factor $(1 + z)$ to yield $f_{\text{em}}(500)$ as

$$f_{\text{em}}(500) = 10^{-26} S(178) \left(\tfrac{500}{178}\right)^{\alpha} (1 + z)^{-(1+\alpha)},$$ (7)

---

[2] Throughout this paper flux densities are in W m^{-2} (c/s)$^{-1}$, i e , per unit frequency; it is only for convenience of notation that in the optical range wavelength in angstroms is used as the argument.

where $S(178)$ is the corrected flux density in flux units $(10^{-26}$ W m^{-2} (c/s)$^{-1})$. We drop the subscript of $f(500)$ and list the derived values in Table 1.

Figure 3 shows the redshift–radio magnitude diagram for the forty 3CR sources. Bolton (1966) and Roeder and Mitchell (1966) have suggested that the apparent lack of a redshift-magnitude relation (Hoyle and Burbidge 1966) is due to the large dispersion of the absolute radio luminosities.

VI. DISTRIBUTION IN SPACE

The identifications of QSS in the *3CR Catalogue* (Wyndham 1966; Véron 1966; Sandage and Schmidt 1967) can only be complete down to some limiting optical magnitude. This limiting magnitude is probably between 18 and 19, some 2 mag above the
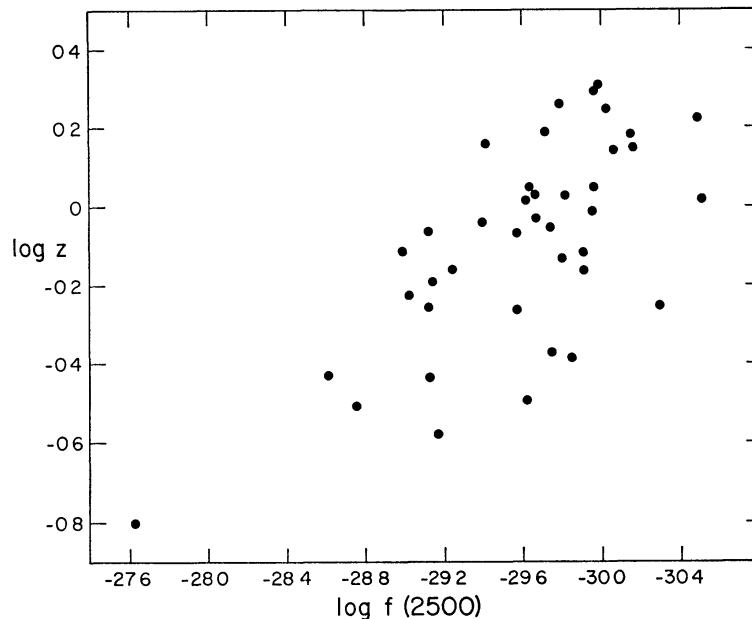

FIG. 2.—Redshift-magnitude diagram for 40 3CR QSS The flux density $f(2500)$ is measured at emitted wavelength 2500 Å over a band width of 1 c/s emitted, in units of W m^{-2} (c/s)$^{-1}$.

limit of the *Palomar Sky Survey*. We have adopted as the limiting optical flux density $\log f(2500) = -30.00$, roughly corresponding to an observed visual magnitude $V \approx 18.4$. There are thirty-three sources brighter than this limit in Table 1.

The *3CR Catalogue* has a well-defined limiting observed flux density of 9×10^{-26} W m^{-2} (c/s)$^{-1}$ at 178 Mc/s. In principle we could convert this to a limiting flux density at the standard emitted frequency of 500 Mc/s, but it would depend strongly on the spectral index and the redshift as can be seen from equation (7). There is, in fact, no need to do so since the procedure developed subsequently in this paper allows the use of a limiting observed flux density.

We are now in a position to study the space distribution of QSS from the thirty-three 3CR sources in our complete sample as defined above. Assuming all along that the redshifts are cosmological, we shall first test whether or not the QSS have a uniform distribution in space. For this purpose it would not be useful to plot just the distances computed from the redshifts: we would find a strong decrease of density with increasing distance simply because our sample includes at small distances a larger range of absolute luminosities than at large distances. A correct procedure would be to investigate the distance distribution of all sources in a narrow range of absolute optical and radio

luminosity out to the limiting distance to which these would be represented in our complete sample. In the present case this is not feasible, as the number of sources in the sample is small and the range in absolute optical and radio luminosity is large.

The following method for testing uniformity of space distribution turns out to be very suitable for samples limited in flux density. We compute for each source the maximum redshift at which it would still be included in our complete sample. This establishes a maximum volume V_m over which this source could be observed. The actual redshift at which the source is observed similarly corresponds to a volume V. The ratio V/V_m is a measure of the position of the source within the observable volume V_m. The test for uniformity is simply that V/V_m has a uniform distribution from 0 to 1 for the total sample of sources, or that $\langle V/V_m \rangle = \frac{1}{2}$.
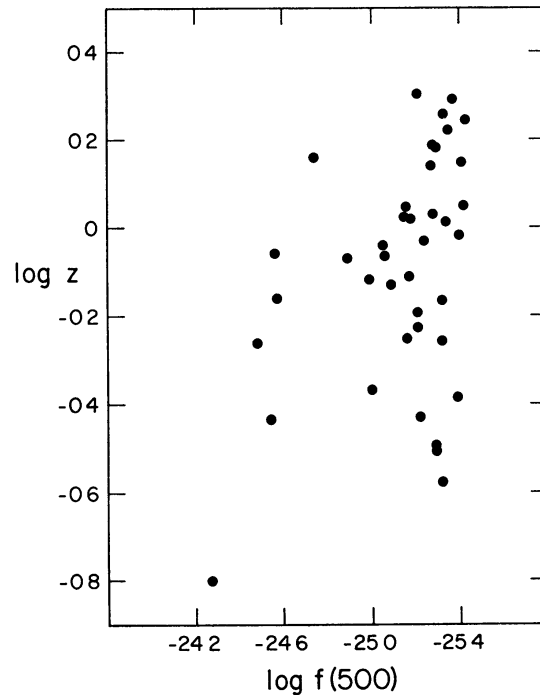

Fig. 3.—Redshift–radio magnitude diagram for 40 3CR QSS. The flux density $f(500)$ is measured at emitted frequency 500 Mc/s over a band width of 1 c/s emitted, in units of W m^{-2} (c/s)$^{-1}$.

We have used relativistic cosmological models of the Universe with zero pressure, zero cosmological constant, a Hubble constant $H_0 = 100$ km sec^{-1} Mpc^{-1}, and a deceleration parameter q_0 (Sandage 1961). The absolute luminosity of the sources in W(c/s)$^{-1}$ is computed from

$$\log F(2500) = \log f(2500) + 2 \log A + 53.03 , \tag{8}$$

and its equivalent for $F(500)$. Here the "luminosity distance" A depends on redshift z and deceleration parameter q_0 (Sandage 1961):

$$A = q_0^{-1}z + q_0^{-2}(q_0 - 1)[\sqrt{(1 + 2q_0 z)} - 1] . \tag{9}$$

Luminosities are given in Table 5 for $q_0 = 0$, in which case $A = z(1 + \frac{1}{2}z)$. Table 6 gives luminosities for $q_0 = 1$, for which $A = z$. Volumes in co-moving coordinates as a function of redshift or luminosity distance are given as numbers $N(m)$ in Table 3 of Sandage (1961). One unit of $N(m)$ corresponds to 5.67×10^5 Mpc^3 over the entire sky.

The optical limiting luminosity distance $A_m{}^{\mathrm{opt}}$ for each source is computed from equation (8), using the limiting flux density $\log f(2500) = -30.00$. The radio limiting luminosity distance $A_m{}^{\mathrm{rad}}$ is computed from equation (7) using the corrected flux density limit $S(178) = 1.16 \times 9$ flux units, and from the radio equivalent of equation (8). Values of $A_m{}^{\mathrm{opt}}$ and $A_m{}^{\mathrm{rad}}$ for each source are given in Tables 5 and 6. The smaller of the two is used to compute the effective limiting volume V_m, which is required to derive V/V_m for each source.

TABLE 5

ABSOLUTE FLUXES AND DATA RELATED TO THE DENSITY DISTRIBUTION ($q_0 = 0$)

Source	log $F(2500)$	log $F(500)$	log $A_m{}^{\mathrm{opt}}$	log $A_m{}^{\mathrm{rad}}$	V/V_m	$V'/V_m{}'$	$(V_m{}')^{-1}$ $(10^{-12}\ \mathrm{Mpc}^{-3})$
3C 273 .	23 87	27 23	+0 420	−0 299	0 07	0 02	71
323 1	22 81	26 66	− .110	− .524	1 00	1 00	450
249 1	23 40	26 86	+ 185	− .388	0 74	0 63	149
277 1	22 55	26 88	− .240	− 366	0 71	0 58	127
48	23 19	27.77	+ 080	+ .030	0 16	0 03	3 9
351 .	23 71	27 10	+ 340	− 308	0 78	0 66	78
215 .	22 58	27 03	− .225	− 281	0 89	0 81	61
47	22 72	27 46	− 155	− 106	0 52	0 32	21
147 .	23 14	28 23	+ .055	+ 286	0 38	0 14	3 1
334	23 61	27.41	+ .290	− 128	0 90	0 82	16
345	23.79	27 60	+ .380	− 084	0 88	0 77	11
263	23 75	27 68	+ 360	+ .010	0.70	0 48	4 7
207 .	23 05	27 64	+ .010	− .012	0 89	0 79	5 7
380	23 73	28 40	+ .350	+ 394	0 21	0 03	0 18
254	23 23	27 94	+ .100	+ .165	0 66	0 40	2 0
138 .	23 16	28 08	+ 065	+ .197	0 83	0 66	2 8
175 .	24 09	27 91	+ .530	+ .152	0 59	0 30	1 2
286 .	23 63	28 31	+ .300	+ 311	0 42	0 12	0 29
454 3	24 09	28 15	+ .530	+ 222	0 59	0.28	0 62
196	23 48	28.66	+ 225	+ 527	0.60	0 29	0 60
309 1	23 87	28 21	+ .420	+ .270	0 55	0 23	0 39
336	23 62	28 05	+ 295	+ .217	0 71	0 44	0 65
288 1	23 39	27 94	+ 180	+ 164	0 96	0 90	1 1
245	23 80	28 07	+ .385	+ 199	0 97	0 93	0 78
287	23 64	28 30	+ .305	+ 320	0 69	0 38	0 27
186	23 79	28 17	+ 380	+ 294	0 73	0 45	0 30
208	23 87	28 34	+ 420	+ 362	0 63	0 29	0 16
204	23 54	28 08	+ 255	+ 244	0 98	0 94	0 50
298	24 41	29 08	+ .690	+ 735	0 37	0 04	0 006
205	24 18	28 61	+ 575	+ 502	0 79	0 49	0 036
432	24 31	28 77	+ .640	+ 586	0.85	0 58	0 016
191	24 24	28 83	+ .605	+ .621	0.94	0 81	0 013
9 .	24 26	29 03	+0.615	+0.714	0.97	0 91	0 010

The distribution of V/V_m for the sample is not at all uniform: only six of the thirty-three sources have a V/V_m less than 0.50. The mean value of V/V_m is 0.69 for $q_0 = 0$, 0.70 for $q_0 = 1$. It depends little on the value of q_0: for $q_0 = 13$ the mean V/V_m is 0.73.

Next we investigate whether $\langle V/V_m \rangle$ depends on the absolute radio and optical luminosity. We divide the sources in two equal groups, one containing the strong sources, the other the weaker sources. The mean values of V/V_m found are shown in Table 7. We see that $\langle V/V_m \rangle$ for the strong sources (either radio or optical) is around 0.04 smaller than for the weaker sources. In view of the small number of sources this difference is statistically not significant.

The non-uniform distribution of V/V_m, independent of absolute radio or optical luminosity, indicates a strong increase of the density of quasi-stellar sources at large

distance. Our next step is to derive a function $V'(z)$ or $V'(A)$, where V' is the apparent volume, such that V'/V_m' for our sources shows a uniform distribution. Since for small z, $V \sim A^3 (1 + A)^{-3}$ independent of q_0 (Sandage 1961), it seemed natural to try $V' \sim A^3 (1 + A)^{-3+n}$, thus insuring a smooth behavior of V'/V for small redshift, i.e., locally. For $n = 5$, the distribution of V'/V_m' of our sources becomes quite uniform, the mean V'/V_m' being 0.50 for $q_0 = 0$, 0.51 for $q_0 = 1$, and 0.53 for $q_0 = 13$.

We adopt $V' \sim A^3 (1 + A)^2$ as the apparent volume in which the distribution of QSS is uniform, practically independent of q_0. The uncertainty corresponding to the small statistical sample that we have used corresponds to at least one power of $(1 + A)$

TABLE 6

ABSOLUTE FLUXES AND DATA RELATED TO THE DENSITY DISTRIBUTION ($q_0 = 1$)

Source	log $F(2500)$	log $F(500)$	log A_m^{opt}	log A_m^{rad}	V/V_m	V'/V_m'	$(V_m')^{-1}$ $(10^{-12}\,\mathrm{Mpc^{-3}})$
3C 273	23 80	27 16	+0 385	−0 328	0 08	0.02	91
323.1	22 70	26 55	− 165	− 578	1 00	1 00	690
249 1	23 27	26 73	+ 120	− 453	0 76	0 65	257
277 1	22 42	26 75	− .305	− 431	0 72	0 60	214
48	23 04	27 62	+ 005	− 037	0 17	0 03	7 1
351	23 56	26 95	+ 265	− 382	0 78	0 67	143
215	22 42	26 87	− .305	− 361	0 89	0 81	120
47	22 55	27 29	− .240	− 187	0 54	0 33	43
147	22 93	28 02	− .050	+ 199	0 40	0 15	8 1
334	23 40	27 20	+ 185	− 233	0 90	0 82	51
345	23 56	27 37	+ .265	− 198	0 88	0 79	30
263	23 51	27 44	+ .240	− 109	0 70	0 48	14
207.	22 79	27 38	− 120	− 142	0 91	0 81	18
380	23 47	28 14	+ 220	+ 274	0 26	0 03	0 62
254	22 96	27 67	− 035	+ 031	0 67	0 41	7 1
138	22 88	27 80	− 075	+ 064	0 84	0 67	10
175	23 81	27 63	+ 390	+ 012	0 61	0 32	4 6
286 .	23 32	28 00	+ 145	+ 176	0 46	0 13	1 3
454 3	23 78	27 84	+ 375	+ 076	0 59	0 27	2 5
196	23 17	28 35	+ 070	+ 385	0 62	0 30	2 7
309 1	23 55	27 89	+ 260	+ 120	0 56	0 22	1 7
336	23 29	27 72	+ 130	+ 053	0 73	0 45	3 1
288 1	23 05	27 60	+ 010	− 006	0 96	0 91	5 4
245	23 44	27 71	+ 205	+ 020	0 97	0 93	4 2
287	23 27	27 93	+ 120	+ 142	0 72	0 40	1 7
186	23 42	27 80	+ 195	+ 108	0 76	0 47	1 9
208	23 49	27 96	+ 230	+ 174	0 65	0 29	1 0
204	23 16	27 70	+ 065	+ 054	0 97	0 93	3 1
298	23 94	28 61	+ 455	+ 503	0 46	0 05	0 06
205	23 69	28 12	+ 330	+ 258	0 81	0 49	0 43
432	23 75	28 21	+ 360	+ 306	0 89	0 61	0 27
191	23 65	28 24	+ 310	+ 327	0 95	0 82	0 26
9	23 66	28 43	+0 315	+0 414	0 97	0 90	0 25

TABLE 7

AVERAGE V/V_m VALUES OF WEAK AND STRONG SOURCES

	Radio Weak	Radio Strong	Optical Weak	Optical Strong
$q_0 = 0$	0 71	0 67	0 71	0 66
$q_0 = 1$	0 73	0 68	0 72	0 69

in the proposed expression for V'. For small redshifts our apparent volume V' is $(1 + A)^5$ times the volume V given by the cosmological models considered; for larger redshifts the excess ratio is less than $(1 + A)^5$. The density $\rho(z)$, expressed in the local density, $\rho(z = 0)$, is easily derived; some values are given in Table 8.

It has usually been considered that the steep slope of the $N(S)$ relation of extra-galactic radio sources could be due to an increase with increasing redshift of either the density or the luminosity of the sources (see Oort 1961; Longair 1966a). The case of a luminosity increase is actually a special case of a luminosity-dependent variation, such that the density increases for the high luminosities and decreases for low luminosities. We have seen above that the density increase with increasing redshift of the QSS is independent of luminosity; hence, there is no evidence for luminosity evolution of these sources.[3]

The $N(S)$ slope that corresponds to $V' \sim A^3(1 + A)^2$ is $\frac{3}{2} + A/(1 + A)$, or 1.83 for $A = 0.5$, 2 for $A = 1$, and 2.17 for $A = 2$. Since most 3CR QSS are in this range of A, their $N(S)$ slope is around 2. This is in good agreement with the observed slope for extragalactic radio sources of 1.8 (Scott and Ryle 1961) if we remember that these

TABLE 8

Space Density of QSS, Relative
to the Local Density

z	$\rho(z)/\rho(0)$		
	$q_0 = 0$	$q_0 = 1$	$q_0 = 13$
0 2	3 5	3 3	2 6
0 5	18	14	7
1 0	150	80	25
1 5	800	290	63

include the radio galaxies which have smaller redshifts than the QSS and hence will contribute a smaller slope. There is, in fact, no clear evidence at present whether the radio galaxies show any increase of density with redshift.

VII. OPTICAL AND RADIO LUMINOSITY FUNCTIONS

Let Φ ($\log F$) be the optical luminosity function, defined as the local ($z = 0$) space density of sources of optical luminosity F, per interval $\Delta \log F = 0.4$ ($= 1$ mag). We similarly define the radio luminosity function Ψ ($\log F$).

A luminosity function is usually derived by grouping the sources in the complete sample in intervals of 1 mag of absolute luminosity and by dividing by the volume over which each luminosity group is completely represented in the sample. Alternatively, we can compute the contribution from each source separately by dividing unity by the volume over which it could be observed in the sample and then group in magnitude intervals of absolute magnitude. This alternate method is the only feasible one for our present case in which the surveyable volume depends on both optical and radio luminosity.

We list for each of the thirty-three sources of our sample the value of $(V_m')^{-1}$. The

[3] It is preferable to use $\langle V'/V_m' \rangle$ rather than $\langle V/V_m \rangle$ to study the dependence of the density increase on luminosity. While $\langle V'/V_m' \rangle = 0.51$ for $q_0 = 1$ for all sources, it is 0.54 for the optically weak ones and 0.61 for the radio weak ones. The latter value suggests that the density of the weak radio sources increases more rapidly with redshift than that of the strong radio sources; however, the statistical significance of the difference is marginal.

luminosity functions, both optical and radio, are obtained by collecting the sources in groups of 1 mag (0.4 in log F, either optical or radio, respectively) and summing the $(V_m')^{-1}$ values in each group. We have assumed that our sample of thirty-three sources represents 43 per cent of the sky. This estimate is based on the area covered by the *3CR Catalogue* (above declination $-5°$), the effect of galactic obscuration (none of our sources is at a galactic latitude less than 10°) and the likelihood that 3C 93 (which shows a lineless spectrum) would qualify for the complete sample.

TABLE 9

LUMINOSITY FUNCTIONS* FOR $q_0 = 0$ FOR SOURCES WITH
LOG $F(2500) > 22.5$, LOG $F(500) > 26.5$

log $F(2500)$	$\Phi(\log F)$ (10^{-12} Mpc^{-3})	log $F(500)$	$\Psi(\log F)$ (10^{-12} Mpc^{-3})
24 1–24 5 . ..	0 081	28 9–29 3. ..	0 016
23 7–24 1 . .	168 33	28.5–28 9..	0 665
23 3–23 7	168 41	28 1–28 5	5 31
22 9–23 3	17 5	27.7–28 1 .	12 93
22 5–22 9. . ..	659	27.3–27.7....	58 4
		26 9–27 3...	210
		26.5–26 9.. ..	726

* The accuracy of the values given for the luminosity functions is quite low; the several decimal places are only given to maintain consistency with data from Table 5.

TABLE 10

LUMINOSITY FUNCTIONS* FOR $q_0 = 1$ FOR SOURCES WITH
LOG $F(2500) > 22.4$, LOG $F(500) > 26.4$

log $F(2500)$	$\Phi(\log F)$ (10^{-12} Mpc^{-3})	log $F(500)$	$\Psi(\log F)$ (10^{-12} Mpc^{-3})
23 6–24 0 . . .	99 37	28 4–28 8....	0 31
23 2–23 6 .	510.52	28 0–28 4 . .	12 98
22 8–23 2 .	43 5	27 6–28 0 .	51 1
22 4–22 8 . .	1085	27 2–27 6	133
		26 8–27 2 . .	380
		26 4–26 8 ..	1161

* See note to Table 9.

The luminosity functions are given in Tables 9 and 10. The optical luminosity function shows large fluctuations suggesting a distribution with two maxima. However, the statistical uncertainty would allow a fairly flat luminosity function just as well.

The radio luminosity function shows a continuous increase toward fainter luminosities, by a factor of around 3–4 per mag.

The total local space density of QSS of the luminosity ranges indicated in Tables 9 and 10 is 1.0×10^{-9} Mpc^{-3} for $q_0 = 0$, 1.7×10^{-9} Mpc^{-3} for $q_0 = 1$.

A lower limit to the total number of QSS in the *3CR Catalogue* (i.e., of all optical magnitudes) is derived by counting every source of the complete sample as V_m'(radio)/V_m' sources. This follows immediately from the fact that the radio catalogue and our complete sample survey volumes that are exactly in this ratio. We find a total of sixty-nine QSS for $q_0 = 0$, seventy-one for $q_0 = 1$. The major contributions are from 3C 446 for which V_m'(radio)/$V_m' = 22$, and from 3C 147 for which it is 10. Except for

the corresponding statistical uncertainty, the estimated number of some seventy QSS in the *3CR* is an underestimate, since it does not include sources that are intrinsically weaker, either optical or radio, than all the sources in our sample.

A lower limit to the total number of QSOs (i.e., without any restriction on the radio flux density) brighter than visual magnitude 18.4 over the entire sky is found by counting each source in the complete sample as V_m'(optical)/$(0.43\ V_m')$ objects. The total number so found is 4000 for $q_0 = 0$, and 3500 for $q_0 = 1$. The contribution by 3C 273 is about one-half of these total numbers, so the uncertainty of these numbers is at least 50 per cent. Apart from this large uncertainty, these predicted numbers of QSOs must again be underestimates, since they do not include objects of low optical or radio luminosity. The steepness of the radio luminosity function suggests that these numbers would go up by a factor of around 3 or 4 for every magnitude added to the faint end of the radio luminosity function.

The required amount of extrapolation of the radio luminosity function can be estimated from the actual number of QSOs, which according to Sandage and Luyten (1967) is about 0.4 per square degree down to $B = 18$. Further data on the photometry kindly made available by Dr. Sandage suggest a number of about 0.3 per square degree down to $V = 17.9$. From this we may estimate that there are some 26000 QSOs down to $V = 18.4$ over the entire sky. This is around 7 times our estimate based on a radio luminosity function down to around log $F(500) = 26.5$. Extrapolation of the radio luminosity function with the observed slope down to about log $F(500) = 25.9$ would be sufficient to explain the observed frequency of QSOs. The total local space density QSOs is then 7×10^{-9} Mpc^{-3} $(q_0 = 0)$, 12×10^{-9} Mpc^{-3} $(q_0 = 1)$.

A similar extrapolation of the radio luminosity function has been proposed by Braccesi, Fanti, Giovannini, and Vespignani (1966) on the basis of a search for radio emission from QSOs. However, observations by Fanti-Giovannini and Fanti (1967) of further QSOs gave no detectable radio emission. Much further observational work at low flux densities will be required to gain information about the faint end of the radio luminosity function.

VIII. DISCUSSION

The main results of our investigation are (*a*) that the number of QSS within "luminosity distance" A is $N \sim A^3(1 + A)^2$ independent of absolute luminosity; (*b*) the local density of QSOs of all radio luminosities is $7 - 12 \times 10^{-9}$ Mpc^{-3}; (*c*) the optical luminosity function is probably fairly flat; and (*d*) the radio luminosity function shows a strong increase toward lower radio luminosities.

The above results are still tentative as they depend on a sample of only thirty-three 3CR sources. The following remarks discuss some of the aspects of our derivation and other points of interest.

1. Many QSS show optical variability, typically of 0.3 mag. The effect of this variability on the parameter V/V_m is small, and mostly of a random character.

2. The choice of log $f(2500) = -30.00$ as the limit above which our sample is complete may have been incorrect. However, if there are some sources just above this flux limit missing from our sample, then our derived value of $\langle V/V_m \rangle$ is an underestimate, since the missing sources would have a V/V_m close to unity. Hence, if our sample is incomplete at the faint end then the density increase with redshift is larger than that derived.

3. The mean values of V/V_m found in § VI depend little on q_0. In the case of the steady-state theory, corresponding to $q_0 = -1$, it is more meaningful to work with the parameter N/N_m, where N is the number of galaxies up to a given redshift, since N includes the effect of continuous creation. The value of N/N_m found for our sample of thirty-three 3CR sources is 0.75. This is in direct conflict with the value of 0.50 required by a steady state in which no evolutionary effects are admitted.

4. Our claim that the density increase toward large redshifts is independent of luminosity was based on the constancy of $\langle V/V_m \rangle$ (see Table 7). Admittedly, the mean V/V_m for the weaker sources refers to a smaller mean redshift than that for the bright sources. Hence the density increase with redshift of weak sources is established out to a rather smaller redshift than that for the brighter sources. We cannot therefore exclude that at, say, $z > 1$, the density increase of weak sources becomes different from that of bright sources, but it would be artificial to make such an assumption without further evidence.

5. It should be stressed again that the form of $N(A)$ adopted, namely, $A^3(1 + A)^2$, is rather arbitrary, and that the uncertainty amounts to at least one power of $(1 + A)$. It is a definite advantage of this form of $N(A)$ that it depends little on the value of q_0, as may be seen from the results given in § VI for the very large range of q_0 from 0 to 13. No cosmological models with a non-zero cosmological constant have been considered in this investigation. Finally, the relation $N \sim A^3 (1 + A)^2$ will have to be cut off at some value of A to avoid an integrated brightness larger than that observed for the colder parts of the radio sky and to account for the observed flattening of the $N(S)$ relation at low flux density (Longair 1966a).

6. Evolution, i.e., dependence on redshift, of any intrinsic optical or radio property may be investigated through V/V_m or V'/V_m'. There is marginal evidence that the spectral index α shows an evolution effect: the mean V/V_m seems to be larger for steeper radio spectra. This would indicate a larger density increase with redshift for the steeper spectra. Larger samples will be required to check this suggestion.

7. It is not clear yet whether or not optical and radio luminosity are independent. If they are not independent, then the optical luminosity function as derived applies only to sources with a mean radio luminosity equal to that of the thirty-three 3CR sources, and vice versa. The extrapolation of the radio luminosity function to include all QSOs (see § VII) would be affected by a dependence of optical and radio luminosity.

8. If the density increase with redshift is entirely independent of optical and radio luminosity, then the QSOs should show a correspondingly steep increase of numbers with optical magnitude. Optical surveys of QSOs complete down to magnitude 18 or fainter over limited areas of the sky will yield the required information.

APPENDIX

REDSHIFTS OF SIXTEEN QUASI-STELLAR RADIO SOURCES

The sources are listed in order of redshift in Table A1 together with references for the identifications. The source 4C 29.50 has been identified by J. D. Wyndham with a stellar object of magnitude 19 at $\alpha(1950) = 17^h02^m10^s7$, $\delta(1950) = +29°51'01''$. I am grateful to all the authors referred to in Table A1 for early communication of identification data.

The observing equipment and the procedure used to identify the emission lines are identical to those of Schmidt (1965, 1966). The spectra of AO 0952+17 and 4C 29.50 are on baked Eastman IIaO plates, limiting the spectral regions to about 3200–4950 Å. All other spectra reach to 6300 Å, at least. Most of the emission lines show apparent widths of around 30 or 40 Å.

The redshifts $z = (\lambda - \lambda_0)/\lambda_0$ and the computed rest wavelengths of the lines are given in Table A2. Further remarks for the individual sources are given below.

4C 01.4: The redshift agrees well with those determined by Lynds (1967) and Kinman and Burbidge (1967).

3C 323.1: The [O III] $\lambda\lambda4959$, 5007 are unresolved, hence less than 10 Å wide, the width of

TABLE A1

WAVELENGTHS OF EMISSION LINES

Source	Reference for Identification*	λ(Å)†
4C 01.4=PHL 1093	(1)	3530 m, 4318 m, 6123 w
3C 323 1....	(2)	3540 m, 5519 w, 6141:s, 6266 w, 6330 m
4C 15 1=PHL 658	(1)	4061 m, 5404 w, 5621 w, 5958:w
3C 232	(3)	4292 s, 4508 m, 5703 w, 5925:w, 6644:w
3C 57=PKS 0159−11	(4)	3197:w, 4674 m, 6226:w
4C −00.6=PHL 923	(1)	3289 w, 4812 m
3C 454 3 .. .	(5)	3552 w, 5201 w
3C 309 1 .. .	(2)	3642 m, 5337 m
3C 288 1 .. .	(2)	3745 w, 5487 w
3C 268 4	(2)	3722 s, 4578 m
4C −04 6=PHL 1377	(1)	3787 m, 4665 m
AO 0952+17 ..	(6)	3828 m, 4724 m
3C 205... .	(2)	3922 m, 4164 w, 4827 w
4C 29.50.	(7)	3560 s, 4533 s
4C −04 8=PHL 1305	(1)	3721 m, 4746 w
PKS 0229+13 .	(8)	3728 s, 4751 s

* *References:* (1) Scheuer, P. A. G , and Wills, D. 1966, *Ap. J.*, **143**, 274; (2) Wyndham, J D. 1966, *Ap J* , **144**, 459; (3) Wade, C M., according to Sandage, A. R 1966, *Ap. J.*, **146**, 13; (4) Bolton, J G , Shimmins, A. J., Ekers, J., Kinman, T. D., Lamla, E , and Wirtanen, C A. 1966, *Ap. J.*, **144**, 1229; (5) Sandage, A R. 1966, *Ap J.*, **144**, 1234; (6) Hazard, C. 1965 (private communication); (7) Wyndham, J. D 1966 (private communication); (8) Kinman, T D., Bolton, J. G , Clarke, R W , and Sandage, A R 1967, *Ap J* , **147**, 848

† The strength of the emission lines relative to the continuum is indicated by the symbols "w" (weak), "m" (medium), and "s" (strong).

TABLE A2

REDSHIFTS, LINE IDENTIFICATIONS, AND COMPUTED REST WAVELENGTHS

Source	z	Ly-α λ1216	C IV λ1549	C III λ1909	Mg II λ2798	[Ne v] λ3426	[O II] λ3727	Notes*
4C 01.4. ...	0 261				2799	3424		(1)
3C 323.1 . .	0 264				2801	.	...	(2)
4C 15.1 ...	0 451				2799		3724	(3)
3C 232 ..	0 532			.	2802		3723	(4)
3C 57.. . .	0 670			1914:	2800		3728:	
4C −00.6 ..	0 720			1912	2798			
3C 454 3 . .	0 860			1910	2796			
3C 309 1 ..	0 908			1909	2797			
3C 288 1 ..	0 961		. . .	1910	2798			
3C 268 4 ..	1 400		1551	1908				(5)
4C −04 6 .	1 445		1549	1908				
AO 0952+17	1 472		1549	1911				
3C 205......	1.534	...	1548	1905				(6)
4C 29.50. ..	1 927	1216	1549	.				
4C −04 8 ..	2 062	1215	1550					
PKS 0229+13	2 067	1216	1549	.				

* (1) Also Hβ at computed rest wavelength of 4856 Å
(2) Also Hβ and the [O III] λλ4363, 4959, 5007 lines at computed rest wavelengths of 4858, 4366, 4958, and 5008 Å, respectively.
(3) Also [Ne II] λ3869 and Hδ at computed rest wavelengths of 3874 and 4106, respectively.
(4) Also an unidentified line (see text), [Ne III] λ3869, and Hγ at computed rest wavelengths of 2943, 3867, and 4336 Å, respectively.
(5) Suspected emission at 3934 Å is most probably He II λ1640.
(6) Also He II λ1640 at computed rest wavelength 1643 Å

[O III] λ4363 cannot be judged due to its faintness. The Mg II and Hβ lines are at least 50 Å wide.

4C 15.1: Redshift in good agreement with Lynds (1967), though mostly from different lines.

3C 232: The rest wavelengths of four lines fit quite well, even though the lines at 5925 and 6644 Å are uncertain. With the redshift of 0.532, the line observed at 4508 Å has a computed rest wavelength of 2943 Å. No reasonable identification at this wavelength has been found. The possibility that this line is Mg II emission at a redshift of 0.61 cannot be ruled out at present.

3C 57: This is a difficult object, only the line at 4674 Å being easily detectable. Dibai and Esipov (1967) identified emission seen at about 4700 Å and 6490 Å as Mg II λ2798 and [Ne III] λ3869 at a redshift of 0.68. Apart from an apparent systematic difference in the wavelengths, the agreement in redshift is satisfactory.

4C − 00.6: Redshift in reasonable agreement with Lynds (1967).

3C 454.3: Redshift in agreement with Lynds (1967) and Dibai and Esipov (1967).

3C 309.1: Redshift in reasonable agreement with Burbidge and Kinman (1966) and Lynds (1967).

3C 288.1: Both lines are weak and at least 60 Å wide, but the wavelength fit is good.

3C 268.4: The lines seem to have a central core less than 20 Å wide.

4C − 04.6: The wavelengths differ systematically from those given by Kinman and Burbidge (1967), who give a redshift of 1.434. Hiltner, Cowley, and Schild (1966) found a redshift of 1.439; their suggestion of an alternate value of 0.354 would require absence of [Ne III], Hδ, and Hγ emission, since these are not seen at the corresponding wavelengths.

AO 0952+17: Redshift agrees with that given by Kinman and Burbidge (1967).

3C 205: This is a difficult object because the C IV emission is cut in two parts by strong absorption, about 30 Å wide. This absorption is some 9 Å to the red of the emission line at observed wavelength 3931 Å, hence z_{abs} = 1.538. This emission redshift is a compromise from weak lines attributed to He II and C III.

4C 29.50: No continuum is seen below Ly-α, but this is entirely due to a somewhat weak exposure of this 19^m object.

4C − 04.8: No He II λ1640 or C III λ1909 emission is seen at the corresponding wavelength. The redshift agrees with Lynds (1967).

PKS 0229+13: There may be weak emission due to Si IV λ1397 or O IV λ1406. No He II or C III emission is seen.

REFERENCES

Bennett, A. S. 1962, *Mem. R.A S.*, **68**, 163.
Bolton, J. G. 1966, *Nature*, **211**, 917.
Braccesi, A., Fanti, R., Giovannini, C., and Vespignani, G. 1966, *Ap J.*, **143**, 600.
Burbidge, E. M. 1965, *Ap. J.*, **142**, 1674.
———. 1966, *ibid.*, **143**, 612.
Burbidge, E. M., and Kinman, T. D. 1966, *Ap. J.*, **145**, 654.
Burbidge, E. M , Lynds, C. R., and Burbidge, G. R. 1966, *Ap. J.*, **144**, 447
Dibai, E. A., and Esipov, V. F. 1967, *Astr. Tsirk. U.S.S.R.*, No. 403.
Fanti-Giovannini, C., and Fanti, R. 1967, *Nuovo Cimento*, **49B**, 154.
Ford, W. K., and Rubin, V. C. 1966, *Ap. J.*, **145**, 357.
Greenstein, J. L., and Matthews, T. A. 1963, *Nature*, **197**, 1041.
Heidmann, J. 1966, *C.R.*, **262**, 1112.
Hiltner, W. A., Cowley, A. P., and Schild, R. E. 1966, *Pub. A.S.P* , **78**, 464.
Hoyle, F., and Burbidge, G. R. 1966, *Nature*, **210**, 1346.
Kafka, P., 1967a, *Nature*, **213**, 346.
———. 1967b, *Institutsbericht Max-Planck-Institut* (preprint).
Kellermann, K. I. 1964, *Ap. J.*, **140**, 969.
Kinman, T. D., and Burbidge, E. M. 1967, *Ap. J.* (*Letters*), **148**, L59.
Longair, M. S. 1966a, *M.N.R.A.S.*, **133**, 421.
———. 1966b, *Nature*, **211**, 949.
Lynds, C. R. 1966, discussion at Byurakan Conference.
——— 1967, *Ap. J.*, **147**, 837.
Lynds, C. R., Hill, S. J , Heere, K., and Stockton, A. N. 1966, *Ap. J* , **144**, 1244.

Lynds, C. R , Stockton, A. N., and Livingston, W. C. 1965, *Ap. J.*, **142**, 1667.
McVittie, G. C., and Stabell, R. 1967, *Nature*, **213**, 133.
Matthews, T. A , and Sandage, A. R. 1963, *Ap. J.*, **138**, 30.
Oke, J. B. 1965, *Ap. J* , **142**, 810.
———. 1966, *ibid.*, **145**, 668.
Oort, J. H. 1961, *O E.C.D Symp. Large Antennae for Radio Astr.* (Paris).
Pauliny-Toth, I. I. K., Wade, C. M., and Heeschen, D. S. 1966, *Ap. J. Suppl.*, **13**, 65.
Roeder, R. C., and Mitchell, G. F. 1966, *Nature*, **212**, 165.
Rowan-Robinson, M. 1966, *Nature*, **212**, 1556.
Sandage, A. R. 1961, *Ap. J.*, **133**, 355.
———. 1965, *ibid* , **141**, 1560.
———. 1966, *ibid* , **146**, 13.
———. 1967 (private communication).
Sandage, A. R , and Luyten, W. J. 1967, *Ap. J* , **148**, 767.
Sandage, A. R., and Schmidt, M. 1967 (in preparation).
Schmidt, M. 1963, *Nature*, **197**, 1040.
———. 1965, *Ap. J* , **141**, 1295.
———. 1966, *ibid.*, **144**, 443.
Schmidt, M., and Matthews, T. A. 1964, *Ap. J.*, **139**, 781.
Sciama, D. W., and Rees, M. J. 1966, *Nature*, **211**, 1283.
Scott, P. F., and Ryle, M 1961, *M N.R.A.S.*, **122**, 389.
Stockton, A. N , and Lynds, C. R. 1966, *Ap. J.*, **144**, 451.
Strittmatter, P. A , and Burbidge, G. R. 1967, *Ap. J.*, **147**, 13.
Véron, P., 1966, *Ann. d'ap.*, **29**, 231.
Wyndham, J D. 1966, *Ap. J* , **144**, 459.